Article

Downscaling of Future Precipitation in China's Beijing-Tianjin-Hebei Region Using a Weather Generator

Yaoming Liao [1,*], Deliang Chen [2], Zhenyu Han [1] and Dapeng Huang [1]

1   National Climate Center, China Meteorological Administration, Beijing 100081, China;
    hanzy@cma.gov.cn (Z.H.); dapenghuang@163.com (D.H.)
2   Regional Climate Group, Department of Earth Sciences, University of Gothenburg,
    40530 Gothenburg, Sweden; deliang@gvc.gu.se
*   Correspondence: lymzxr@cma.gov.cn

Abstract: To project local precipitation at the existing meteorological stations in China's Beijing-Tianjin-Hebei region in the future, local daily precipitation was simulated for three periods (2006–2030, 2031–2050, and 2051–2070) under RCP 4.5 and RCP 8.5 emission scenarios. These projections were statistically downscaled using a weather generator (BCC/RCG-WG) and the output of five global climate models. Based on the downscaled daily precipitation at 174 stations, eight indices describing mean and extreme precipitation climates were calculated. Overall increasing trends in the frequency and intensity of the mean and extreme precipitation were identified for the majority of the stations studied, which is in line with the GCMs' output. However, the downscaling approach enables more local features to be reflected, adding value to applications at the local scale. Compared with the baseline during 1961–2005, the regional average annual precipitation and its intensity are projected to increase in all three future periods under both RCP 4.5 and RCP 8.5. The projected changes in the number of days with precipitation are relatively small across the Beijing-Tianjin-Hebei region. The regional average annual number of days with precipitation would increase by 0.2~1.0% under both RCP 4.5 and RCP 8.5, except during 2031–2050 under RCP 8.5 when it would decrease by 0.7%. The regional averages of annual days with precipitation ≥25 mm and ≥40 mm, the greatest one-day and five-day precipitation in the Beijing-Tianjin-Hebei region, are projected to increase by 8~30% during all the three periods. The number of days with daily precipitation ≥40 mm was projected to increase most significantly out of the eight indices, indicating the need to consider increased flooding risk in the future. The average annual maximum number of consecutive days without precipitation in the Beijing-Tianjin-Hebei region is projected to decrease, and the drought risk in this area is expected to decrease.

Keywords: weather generator; statistical downscaling; daily precipitation; extreme events; Beijing-Tianjin-Hebei region

1. Introduction

China's Beijing-Tianjin-Hebei region, located at 113.06 to 119.88° E, 36.02 to 42.62° N, includes the Beijing and Tianjin municipalities, and 11 other cities in Hebei Province. The region is one of the major grain production areas as well as the largest urban agglomeration in China [1]. The region covers 216,000 km², has a population of 130 million, and accounted for nearly 10% of China's gross domestic product (GDP) in 2017 [2]. The Xiongan New Area in Hebei Province, which has been under construction since 2017 to ease Beijing's non-capital function, is known as a major national element of China's millennium plan [3].

The terrain of the Beijing-Tianjin-Hebei region is high in the northwest and low in the southeast. From northwest to southeast, the region includes the Bashang Plateau, Yanshan Mountains, Taihang Mountains, and Hebei Plain. The annual average precipitation decreases gradually from southeast to northwest. It is more than 600 mm in parts of the Yanshan area and Hebei Plain, and less than 400 mm on the Bashang Plateau. With a warm

temperate monsoon climate in the Beijing-Tianjin-Hebei region, the weather is dry in spring and humid in summer. Natural disasters such as droughts and floods occur frequently, and the ecological environment is relatively fragile [4–9]. Following global warming trends in climate change, climate variability and the uncertainty of climate anomalies are both increasing, causing increasingly frequent extreme weather or climate events in the Beijing-Tianjin-Hebei region [10,11].

Although a lot of research on extreme climate has been undertaken in the past, it is still a challenge to estimate future extreme precipitation at local scales [12–17]. At present, global climate models (GCMs) are the only tools that can be used to simulate how the increase in greenhouse gas concentrations affects the global climate system [18]. However, the resolution of current GCMs in the space is still too coarse to simulate local climate conditions realistically and reliably. Therefore, GCM output is usually converted into more relevant information at the local or regional scales by dynamical or statistical downscaling methods [19]. In China, downscaling using regional climate models or statistical downscaling methods have been developed and applied in many aspects [20–32]. Recently, the National Climate Center of China has produced a 6.25 km high-resolution future climate projection over China, based on RegCM4.4 and five CMIP5 GCMs [33]. The climate-related risks of rainstorm floods, droughts and water shortages, high temperatures, and heavy hazes in the Xiongan New Area were analyzed based on the 6.25 km high-resolution future climate data [34].

However, dynamical downscaling is computationally expensive and still has a fairly large bias, hindering its direct application [35,36]. More importantly, current regional climate models have a spatial resolution that is still too rough for local scales. In contrast, statistical downscaling is flexible and attractive due to its far lower computational demand compared to dynamical downscaling [37] and its ability to provide necessary local scale information. A weather generator (WG) is a stochastic model that can be used to statistically downscale daily weather. In the past, WGs have provided an effective tool to study the impacts of climate on a variety of systems, and to estimate the probability of extreme events [38–40].

As for local spatial scales and daily time scales, there are few studies related to the simulation and analysis of future extreme climate events, especially for the Beijing-Tianjin-Hebei megalopolis. This paper focuses on the projection of future changes in local daily precipitation characteristics across the Beijing-Tianjin-Hebei region, especially extreme precipitation events, based on a statistical downscaling method with a WG and the coarse spatial output of the five selected GCMs.

2. Data and Methods

2.1. Precipitation Data from Observations and GCMs

Daily precipitation observations at 174 meteorological stations in the Beijing-Tianjin-Hebei region from 1961 to 2005 were used. These data were provided by the National Meteorological Information Center of the China Meteorological Administration. Daily precipitation data at each grid box in the past and future under the RCP 4.5 and RCP 8.5 emission scenarios were obtained from five CMIP5 GCMs [41]: CNRM-CM5, CSIRO-Mk3-6-0, EC-EARTH, MIROC-ESM-CHEM, and NorESM1-M, which have been evaluated and selected as the best climate models for northern China [42]. Because the five GCMs use different grid systems, all GCMs data were bi-linearly interpolated to the grid of $1.0°$ lon $\times 1.0°$ lat to facilitate the calculation. The control run from 1961 to 2005 represents past climate and scenarios, while the run from 2006 to 2070 represents future climate conditions. The locations of the meteorological stations and the grid boxes' layout of the GCMs used in the study are shown in Figure 1. The density of stations varies across the region, and is lower in the northern and western mountain areas.
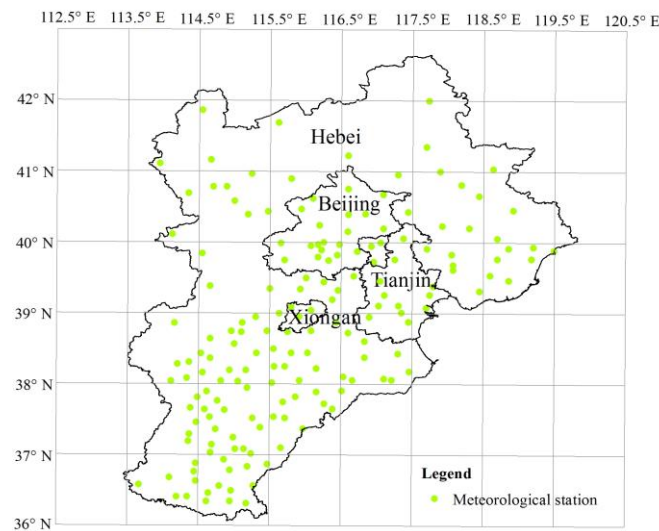
Figure 1. The locations of meteorological stations and the grid boxes' layout of GCMs in the Beijing-Tianjin-Hebei region, China.

2.2. Precipitation Indices

Eight precipitation indices (seen in Table 1) were used in this study to explore various properties of local precipitation in the historical and future periods across the Beijing-Tianjin-Hebei region, focusing on the occurrence and severity of extreme events [43,44]. Generally, the daily precipitation intensity, days of precipitation ≥0.1 mm, and the amount of precipitation are used to represent average precipitation conditions. The numbers of days with precipitation ≥25 mm and ≥40 mm are indices representing rare extreme and very rare extreme precipitation events. The greatest total one-day and five-day precipitation were chosen as short-term and longer-term extremes measures, respectively. Drought risk can be expressed by the maximum number of consecutive days without precipitation.

Table 1. Description of the eight precipitation indices used in the study.

Index	Description (Unit)
Arain	Amount of annual precipitation (mm)
Nrain	Number of days with precipitation ≥0.1 mm (d)
Pint	Daily precipitation intensity (precipitation total per rainy day, mm/d)
Exc25	Number of days with precipitation ≥25 mm (d)
Exc40	Number of days with precipitation ≥40 mm (d)
Px1d	Greatest one-day precipitation (mm)
Px5d	Greatest five-day total precipitation (mm)
Pxcdd	Maximum number of consecutive days without precipitation (d)

2.3. Calculation of WG Parameters

A key component of the downscaling approach in this study is the WG that was used. BCC/RCG-WG was chosen because it has been proven to be skillful in simulating daily variables in China including precipitation, air temperature, sunshine, wind, and relative humidity [45–49]. The BCC/RCG-WG simulates the occurrence and intensity of precipitation at a given station in two separate steps. The first step determines whether a certain day is wet or dry using a two-state, first order Markov Chain. This step involves two transition probabilities: dry day to wet day (Pwd), and wet day to wet day (Pww). The precipitation for a wet day was determined in the second step with a two-parameter (shape parameter alpha and scale parameter beta) gamma distribution function. When simulating daily precipitation, monthly transition probabilities were used in the first step to determine whether a certain day was wet or dry. The precipitation for each wet day was simulated using the monthly parameters of the gamma distribution.

For stochastic generation of precipitation amounts, the parameters for the distribution function should be computed from no fewer than 20 years of historical records [50]. The historical transition probabilities and alpha and beta parameters of 174 stations across the Beijing-Tianjin-Hebei region were calculated for each month using the observed daily precipitation records from 1961 to 2005. The monthly precipitation simulation parameters for each grid box containing at least one precipitation station in the Beijing-Tianjin-Hebei region were computed using daily precipitation data from the control (1961 to 2005) and scenario run (2006 to 2030, 2031 to 2050 and 2051 to 2070). Seven sets of WG parameters for each grid box were produced for each GCM: one set for the control run, and the other six sets for the scenario runs (the two climate scenarios RCP 4.5 and RCP 8.5, and three time periods of 2006–2030, 2031–2050, and 2051–2070).

To project daily precipitations at local stations in the future, it is necessary to determine the parameters that represent the future climate conditions. In this study, local parameters were obtained by assuming uniform changes in parameters for all the stations within a given GCM grid.

$$\frac{WG\_station_{future}}{WG\_station_{observation}} = \frac{WG\_GCM_{scenario}}{WG\_GCM_{control}} \tag{1}$$

This assumption was considered reasonable [51–54], and a new set of future WG parameters was generated in each period for each meteorological station in the region. Overall, a set of 48 parameters was obtained for all stations (four WG parameters for 12 months) for each of the three periods 2006 to 2030, 2031 to 2050, and 2051 to 2070 respectively. These parameters were then used to simulate daily precipitation in the future for those three periods.

2.4. Precipitation Simulation and Future Changes in Indices

Based on the WG parameters for the observed and projected climate, the precipitation at each meteorological station in the past and under the emission scenarios RCP 4.5 and RCP 8.5 for the five GCMs during 2006–2030, 2031–2050, and 2051–2070 were simulated. In order to reasonably represent the climate conditions, 100 years of daily precipitation were simulated. Although historical records cover 45 years and each GCM time span in the future only covers 20 or 25 years, the WG simulated time series for 100 years was used to obtain higher statistical confidence in the simulated precipitation. It is very important when using such simulations to derive statistics for extreme climate events.

All eight precipitation indices in Table 1 were calculated for each meteorological station from the simulation series in the past and under emission scenarios of RCP 4.5 and RCP 8.5 for the five GCMs during the three periods. Then, the relative changes between the observation-based and scenario-based indices under the emission scenarios of RCP 4.5 and RCP 8.5 for five GCMs during the three periods were calculated to quantify the change in the local climate of precipitation.

$$R = \frac{Indice\_Simulation_{future} - Indice\_Simulation_{observation}}{Indice\_Simulation_{observation}} \times 100\% \tag{2}$$

3. Results and Discussion

3.1. Performance of the Precipitation Generator

The simulated precipitation results were compared against the observations to assess the quality of the simulations. Eight indices were derived from the simulated 100 years and compared with the corresponding observed statistics for 1961–2005. The scatter plots in Figure 2 compare the annual indices of precipitation from the observations and simulations. Each dot corresponds to one station. For Arain and Pint, the simulations agreed well with the observed records. The best agreement was achieved for the annual amount of precipitation. For Nrain, the simulations slightly, but systematically, overestimated the number days with precipitation. On the other hand, the simulated extreme indices such as Exc25, Exc40, Px1d, Px5d, and Pxcdd were underestimated at almost all stations. Because

the occurrence of such extreme values is very rare and the historical records are quite short, it is difficult to fit the tail of the gamma distribution function to the observed records [55]. Increasing the length of the historical records would improve the accuracy of parameters calculated from those records, and may improve the simulations.
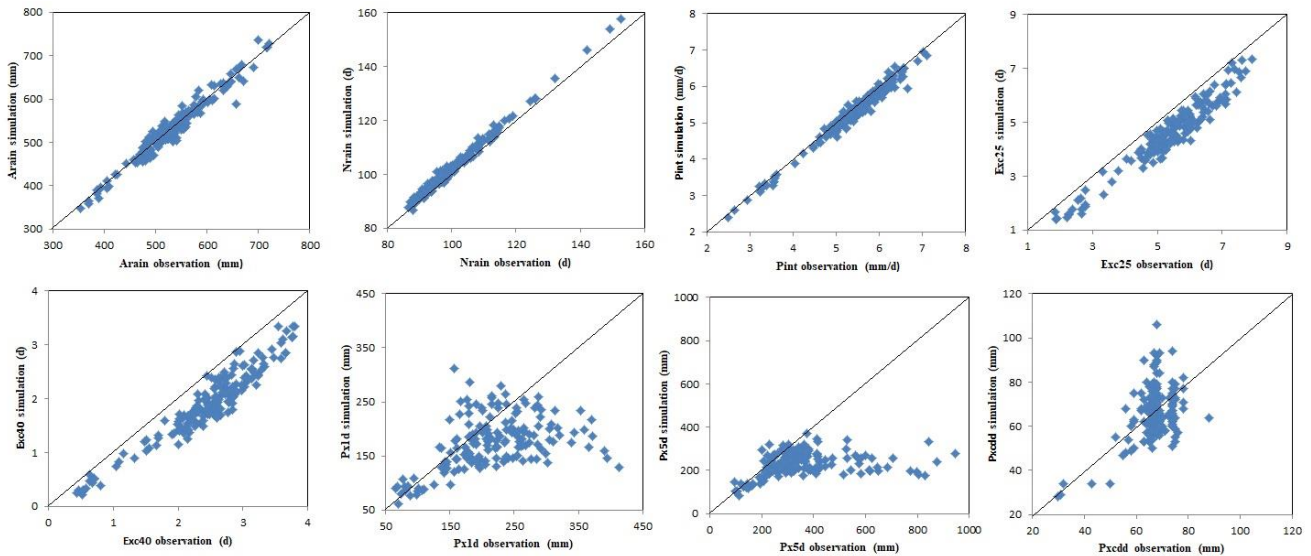
Figure 2. Comparison of the observations and simulations based on the eight precipitation indices. The evaluation is done on an annual scale, each symbol corresponds to one station.

Table 2 shows the regional average percentage changes in the eight precipitation indices in the Beijing-Tianjin-Hebei region during the future three periods calculated from the raw GCM outputs and downscaling data by WG. It can be seen that the changes in the trends of most indices are, in principle, consistent before and after downscaling.

Table 2. Comparison of regional average percentage changes in the eight precipitation indices in the Beijing-Tianjin-Hebei region during the future three periods calculated from the raw GCM outputs and downscaling data by WG (unit: %).

Time Period (Climate Change Scenario)	Data Source	Arain	Nrain	Pint	Exc25	Exc40	Px1d	Px5d	Pxcdd
2006–2030	GCMs	3.2	−1.1	4.5	9.4	21.1	−0.7	5.6	−5.3
(RCP4.5)	Downscaling	7.8	0.2	7.4	14.8	25.4	12.8	14.5	−0.3
2031–2050	GCMs	7.5	0.0	7.5	16.6	31.8	1.0	6.7	−10.2
(RCP4.5)	Downscaling	8.5	0.5	7.9	15.0	21.7	8.3	10.4	−0.5
2051–2070	GCMs	7.6	−0.6	8.3	18.2	39.7	9.0	9.8	−18.0
(RCP4.5)	Downscaling	8.9	0.4	8.3	15.3	23.5	12.6	14.5	−0.2
2006–2030	GCMs	4.4	0.3	4.3	7.7	13.0	-0.7	1.1	−7.0
(RCP8.5)	Downscaling	5.6	0.6	4.9	9.8	17.7	10.8	11.9	−0.5
2031–2050	GCMs	5.8	−0.6	6.5	15.0	27.7	0.9	4.6	−12.6
(RCP8.5)	Downscaling	5.1	−0.7	5.7	10.5	18.4	11.4	12.3	−1.0
2051–2070	GCMs	11.3	−0.5	11.7	30.5	64.9	10.8	16.7	−14.7
(RCP8.5)	Downscaling	10.3	1.0	9.3	18.9	26.3	8.6	9.1	−1.0

3.2. Changes in Precipitation

The percentage changes between the observation-based and scenario-based indices derived from the five GCMs were ensemble averaged to quantify the variation of the precipitation climate in the future. Arain, Nrain, and Pint are the basic indices representing the precipitation conditions. The regional averages of the percentage changes in the three indices simulated by the five GCMs are shown in Table 3, along with their ensemble

mean under the RCP 4.5 and RCP 8.5 emission scenarios. In general, the simulations suggest a change toward a wetter climate at the majority of stations in the Beijing-Tianjin-Hebei region in the future, which is the opposite to the trend in the past [8,56–58], but consistent with most other studies [32,59,60]. Under the influence of global change, with the increasing concentration of greenhouse gases and aerosols, the East Asian summer monsoon is expected to increase, the rain belt in East China may move northward, and the precipitation in North China would increase in summer [61–63]. However, the magnitude and spatial distribution of the changes vary between each of the three indices.

Table 3. Regional average percentage changes in the eight precipitation indices (unit: %), relative to 1961–2005, in the Beijing-Tianjin-Hebei region during the future three periods. These changes were calculated by downscaling from the five GCMs under RCP4.5 and RCP8.5 climate change scenarios.

Time Period (Climate Change Scenario)	GCMs	Arain	Nrain	Pint	Exc25	Exc40	Px1d	Px5d	Pxcdd
2006–2030 (RCP4.5)	CNRM-CM5	16.0	4.9	10.5	22.8	35.4	20.5	23.2	−0.6
	CSIRO-Mk3-6-0	9.7	0.5	9.1	21.7	37.4	15.6	17.1	0.6
	EC-EARTH	4.6	−0.6	5.2	9.1	16.2	7.8	10.9	−1.0
	MIROC-ESM-CHEM	11.5	−0.3	11.9	19.8	34.5	17.8	19.5	−2.5
	NorESM1-M	−3.0	−3.5	0.5	0.5	3.3	2.5	1.9	2.0
	Ensemble Mean	7.8	0.2	7.4	14.8	25.4	12.8	14.5	−0.3
2031–2050 (RCP4.5)	CNRM-CM5	17.9	1.9	15.7	28.5	41.5	20.6	21.3	3.7
	CSIRO-Mk3-6-0	0.3	−1.4	1.8	2.8	8.9	5.0	6.6	2.1
	EC-EARTH	18.1	4.0	13.5	30.3	44.5	16.1	19.7	−2.1
	MIROC-ESM-CHEM	2.8	−2.5	5.5	5.6	8.3	5.1	5.5	−3.6
	NorESM1-M	3.5	0.7	2.8	7.9	5.3	−5.4	−1.0	−2.4
	Ensemble Mean	8.5	0.5	7.9	15.0	21.7	8.3	10.4	−0.5
2051–2070 (RCP4.5)	CNRM-CM5	25.6	6.1	18.3	40.0	56.7	25.9	29.2	−2.1
	CSIRO-Mk3-6-0	−7.1	−2.6	−4.5	−10.5	−5.0	4.5	5.3	1.1
	EC-EARTH	10.7	1.3	9.3	17.6	30.7	21.3	21.2	2.1
	MIROC-ESM-CHEM	6.6	0.8	5.7	8.1	10.1	5.6	8.6	−5.5
	NorESM1-M	8.6	−3.5	12.5	21.1	25.1	5.6	8.0	3.7
	Ensemble Mean	8.9	0.4	8.3	15.3	23.5	12.6	14.5	−0.2
2006–2030 (RCP8.5)	CNRM-CM5	4.7	0.8	3.9	7.3	13.5	9.2	10.1	0.4
	CSIRO-Mk3-6-0	5.8	3.0	2.7	8.1	18.5	12.5	13.0	−3.7
	EC-EARTH	11.7	2.0	9.5	20.2	35.0	18.8	22.0	−2.2
	MIROC-ESM-CHEM	−1.1	−3.5	2.5	0.2	7.0	11.9	10.1	1.2
	NorESM1-M	7.0	0.8	6.1	13.4	14.7	1.4	4.5	1.8
	Ensemble Mean	5.6	0.6	4.9	9.8	17.7	10.8	11.9	−0.5
2031–2050 (RCP8.5)	CNRM-CM5	4.9	1.3	3.5	10.3	16.8	7.8	11.1	−0.9
	CSIRO-Mk3-6-0	6.7	−0.2	6.9	15.1	33.7	17.9	18.7	−4.4
	EC-EARTH	14.3	1.5	12.7	23.8	31.3	17.1	18.1	−0.1
	MIROC-ESM-CHEM	−3.8	−5.9	2.2	−4.7	−6.5	3.0	2.4	0.0
	NorESM1-M	3.2	−0.2	3.4	7.9	16.5	11.3	11.2	0.4
	Ensemble Mean	5.1	−0.7	5.7	10.5	18.4	11.4	12.3	−1.0

Table 3. *Cont.*

Time Period (Climate Change Scenario)	GCMs	Arain	Nrain	Pint	Exc25	Exc40	Px1d	Px5d	Pxcdd
2051–2070 (RCP8.5)	CNRM-CM5	15.6	−0.5	16.3	29.1	35.8	8.2	9.1	-0.2
	CSIRO-Mk3-6-0	1.7	2.9	−0.9	1.4	10.0	9.5	9.0	1.6
	EC-EARTH	13.9	1.3	12.5	27.5	43.5	15.6	17.9	−1.2
	MIROC-ESM-CHEM	3.3	−2.8	6.2	6.0	8.4	6.2	3.0	−3.6
	NorESM1-M	17.0	4.2	12.3	30.3	34.0	3.3	6.6	−1.7
	Ensemble Mean	10.3	1.0	9.3	18.9	26.3	8.6	9.1	−1.0

The annual precipitation tends to decrease during the period 2006–2030 under RCP 4.5 at a few northern stations, and during 2006–2030 and 2031–2050 under RCP 8.5 at a few southern stations. However, the regional average changes in Arain were all positive for the three future periods. Under the RCP 4.5 emission scenario, the average changes projected by the five GCMs during 2006–2030, 2031–2050, and 2051–2070 were 7.8%, 8.5%, and 8.9%, respectively. Amongst the individual GCMs, the results from NorESM1-M for 2006–2030 and from CSIRO-MK3-6-0 for 2051–2070 showed drying trends, which are in contrast to those of most other GCMs. According to the raw data statistics, these two GCMs also showed a drying trend in these two periods. Under the RCP 8.5 emission scenario, annual precipitation in the future also showed an increasing trend. However, the magnitudes of these changes during 2006–2030 and 2031–2050 were 5.6% and 5.1%, respectively, both less than the changes projected under RCP 4.5. The expected change for 2051–2070 was 10.3%, which was more than that for RCP 4.5. The regional average increases over Beijing, Tianjin, and the Xiongan New Area were 12.3%, 11.7%, and 9.3%, respectively (Table 4). Amongst the individual GCMs, the only drying trend was projected by MIROC-ESM-CHEM during 2006–2030 and 2031–2050.

For most GCMs, the number of future precipitation day changed much less than the precipitation amount under both the RCP 4.5 and RCP 8.5 emission scenarios. Some GCMs showed increasing precipitation days, while others showed decreases. Averaged over the five GCMs used, the regional average annual Nrain across the Beijing-Tianjin-Hebei region would increase by 0.2%, 0.5%, and 0.4% during 2006–2030, 2031–2050, and 2051–2070, respectively, under RCP 4.5 when compared to the control period. Under RCP 8.5, the average percentage changes were 0.6%, −0.7%, and 1.0% in the future three periods.

Averaged across the five GCMs, the annual precipitation and rainy days would have an increasing trend in the future at most stations, but the former will increase more than the latter, so annual Pint tends to increase at most stations. The regional average changes were projected to be 7.4%, 7.9%, and 8.3% during 2006–2030, 2031–2050, and 2051–2070, respectively, under RCP 4.5, and 4.9%, 5.7%, and 9.3%, respectively, under RCP 8.5. Therefore, the intensity of precipitation would continue to increase under both emission scenarios. Figure 3 shows the geographical distribution of the average percentage change of annual Pint in the Beijing-Tianjin-Hebei region during the three periods relative to 1961–2005. Annual Pint of most stations showed increasing trends, except for some of the southern stations where there was a decreasing trend during 2006–2030 and 2031–2050 under RCP 8.5. The increase is especially strong during 2051–2070 under RCP 8.5. In this period, the increase is projected to exceed 10% at most northern stations, and the regional average increases over Beijing and Tianjin would reach 11.6% and 11.3%, respectively (Table 4). The increase in precipitation is very beneficial in alleviating the drought and water shortage in the Beijing-Tianjin-Hebei region. However, we need to pay more attention to possible rainstorms, floods, and urban waterlogging disasters in the future [64].
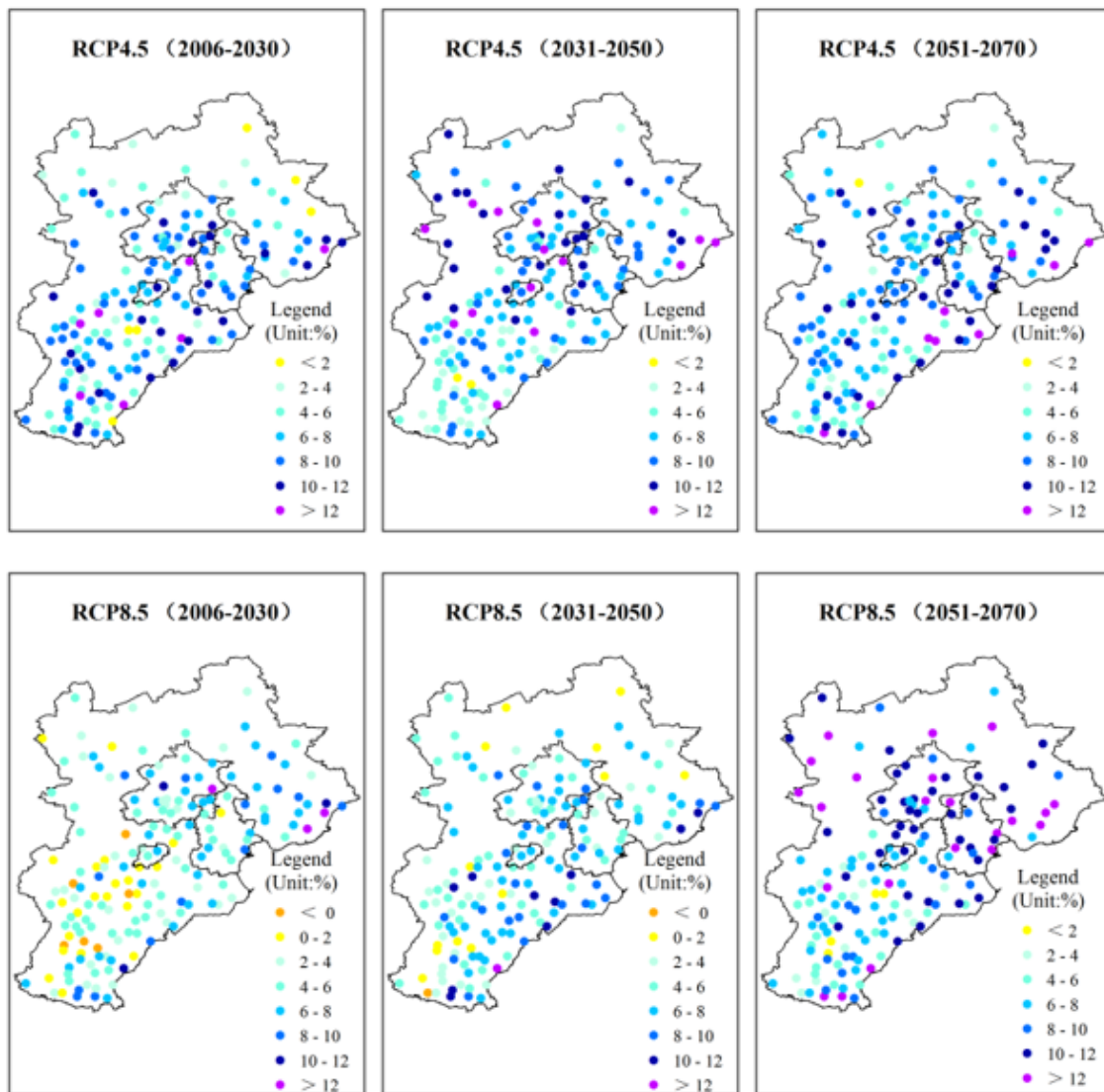
Figure 3. Spatial distribution of annual percentage changes in Pint across the Beijing-Tianjin-Hebei region during 2006–2030, 2031–2050, and 2051–2070, compared with 1961–2005.

Table 4. Regional average percentage changes in the eight precipitation indices during the future three periods in the Beijing, Tianjin, and Xiongan New Area (unit: %).

Time Period (Climate Change Scenario)	Regions	Arain	Nrain	Pint	Exc25	Exc40	Px1d	Px5d	Pxcdd
2006–2030 (RCP4.5)	Beijing	7.5	−0.1	7.5	14.0	21.7	10.3	9.7	−3.2
	Tianjin	8.0	0.1	7.9	12.4	24.1	7.3	16.0	−2.5
	Xiongan New Area	8.4	−0.1	8.5	15.5	29.3	16.8	12.9	8.6
2031–2050 (RCP4.5)	Beijing	8.9	−0.1	9.0	16.4	20.4	4.8	3.2	−0.9
	Tianjin	8.4	0.3	8.0	12.8	18.9	−3.3	5.7	−1.0
	Xiongan New Area	10.8	0.8	9.8	18.6	29.9	11.6	14.4	7.2

Table 4. *Cont.*

Time Period (Climate Change Scenario)	Regions	Arain	Nrain	Pint	Exc25	Exc40	Px1d	Px5d	Pxcdd
2051–2070 (RCP4.5)	Beijing	7.0	−0.8	7.8	13.2	19.7	6.5	10.5	0.5
	Tianjin	8.6	−0.2	8.7	13.3	22.4	2.8	13.1	0.1
	Xiongan New Area	8.4	0.2	7.9	15.4	25.4	12.9	7.9	16.8
2006–2030 (RCP8.5)	Beijing	5.9	−0.2	6.2	11.4	19.6	10.4	11.4	−2.0
	Tianjin	5.9	0.4	5.5	7.7	16.6	0.4	10.6	−0.6
	Xiongan New Area	5.2	0.5	4.8	9.1	18.4	9.8	10.1	1.1
2031–2050 (RCP8.5)	Beijing	4.6	−1.2	5.8	9.5	15.4	9.0	10.1	−2.1
	Tianjin	4.8	−1.0	5.7	7.4	16.0	1.7	13.1	−1.1
	Xiongan New Area	4.8	−1.1	5.9	9.9	19.4	9.4	10.4	1.4
2051–2070 (RCP8.5)	Beijing	12.3	0.6	11.6	22.5	31.5	10.3	13.3	−3.0
	Tianjin	11.7	0.4	11.3	17.9	26.2	1.1	7.2	0.8
	Xiongan New Area	9.3	0.5	8.8	15.6	23.3	7.0	9.7	13.2

3.3. Changes of Extreme Precipitation

Extreme precipitation events can be characterized by indices Exc25, Exc40, Px1d, and Px5d. The regional average percentage changes in the four extreme precipitation indices simulated by the five GCMs and their average under RCP 4.5 and RCP 8.5 are shown in Table 3. Generally, the simulations suggest a change toward more extreme precipitation events across the Beijing-Tianjin-Hebei region in the future. This is consistent with the previous research results [21,32,65]. However, the range and spatial distribution of the changes in the four indices depend on models used and the period analyzed.

Firstly, considering the GCM average Exc25 under RCP 4.5, the changes during 2006–2030, 2031–2050, and 2051–2070 are projected as 14.8%, 15.0%, and 15.3% respectively. The only GCM that shows a decreasing trend in this percentage change is CSIRO-MK3-6-0 during the period 2051–2070. Under RCP 8.5, the number of days with precipitation $\geq$25 mm also shows an increasing trend, but the changes of this index during 2006–2030 and 2031–2050 are 9.8% and 10.5%, respectively, both of which were less than those under RCP 4.5. The change in Exc25 for 2051–2070 was 18.9%, higher than that for RCP 4.5. The only GCM showing a decreasing trend in this index was MIROC-ESM-CHEM during 2031–2050. Figure 4 shows the spatial distribution of changes of Exc25 in the Beijing-Tianjin-Hebei region during the three time periods compared with 1961–2005. Annual Exc25 tended to increase at most stations under RCP 4.5 and RCP 8.5 emission scenarios. In 2051–2070 under RCP 8.5, this index would increase more than 20% in most northern stations, even increasing by more than 50% in some northwest stations. The regional average percentage increase over Beijing reaches 22.5% (Table 4). However, annual Exc25 does tend to decrease at a few central stations under RCP 8.5.
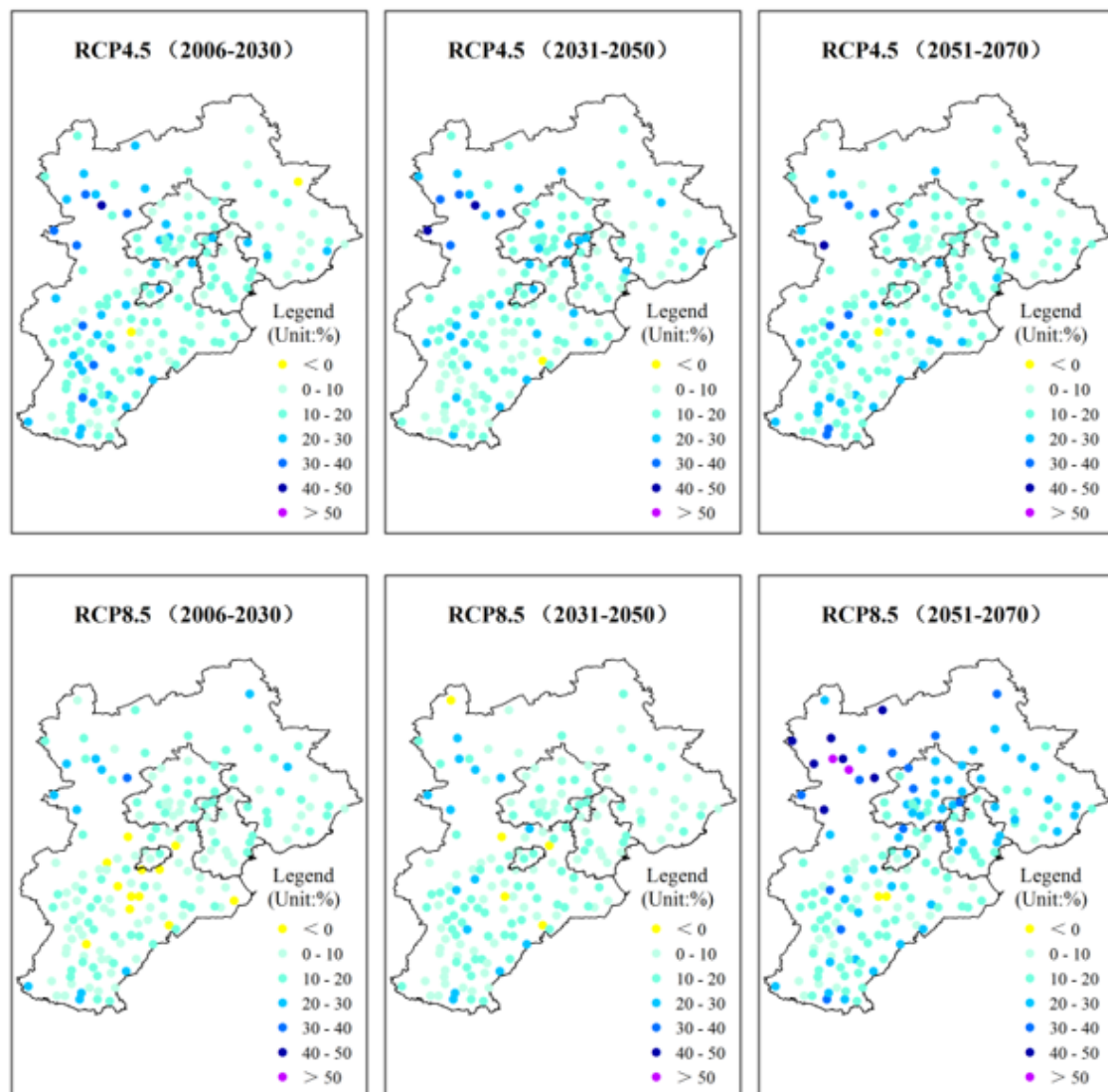
Figure 4. Spatial distribution of annual percentage changes of Exc25 across the Beijing-Tianjin-Hebei region during 2006–2030, 2031–2050 and 2051–2070, compared with 1961–2005.

For most GCMs, the increase in days with precipitation ≥40 mm was obviously greater than the increase in days with precipitation ≥25 mm under both RCP 4.5 and RCP 8.5. Averaged over five GCMs, this increase was the largest among the eight indices. This indicates that rare precipitation events with daily precipitation above 40 mm are expected to occur more frequently in the future. The regional average of annual Exc40 across the Beijing-Tianjin-Hebei region would increase by 25.4%, 21.7%, and 23.5% during 2006–2030, 2031–2050, and 2051–2070, respectively, under RCP 4.5. Meanwhile, under RCP 8.5, the days per year with precipitation ≥40 mm would continue to increase in the future: changes during 2006–2030, 2031–2050, and 2051–2070 would reach 17.7%, 18.4%, and 26.3%, respectively. Figure 5 shows the spatial distribution of percentage changes of Exc40 in the Beijing-Tianjin-Hebei region during the three time periods compared with 1961–2005. Annual Exc40 is projected to increase at most stations in the future, especially at some northwest stations, where the magnitude of the increase is greater than 50%. The northwest Beijing-Tianjin-Hebei region is mainly mountainous, and thus more attention should be paid to the prevention of mountain torrents caused by heavy rainfall in the future [32]. There are only a few stations where the annual Exc40 is projected to decrease in the future.
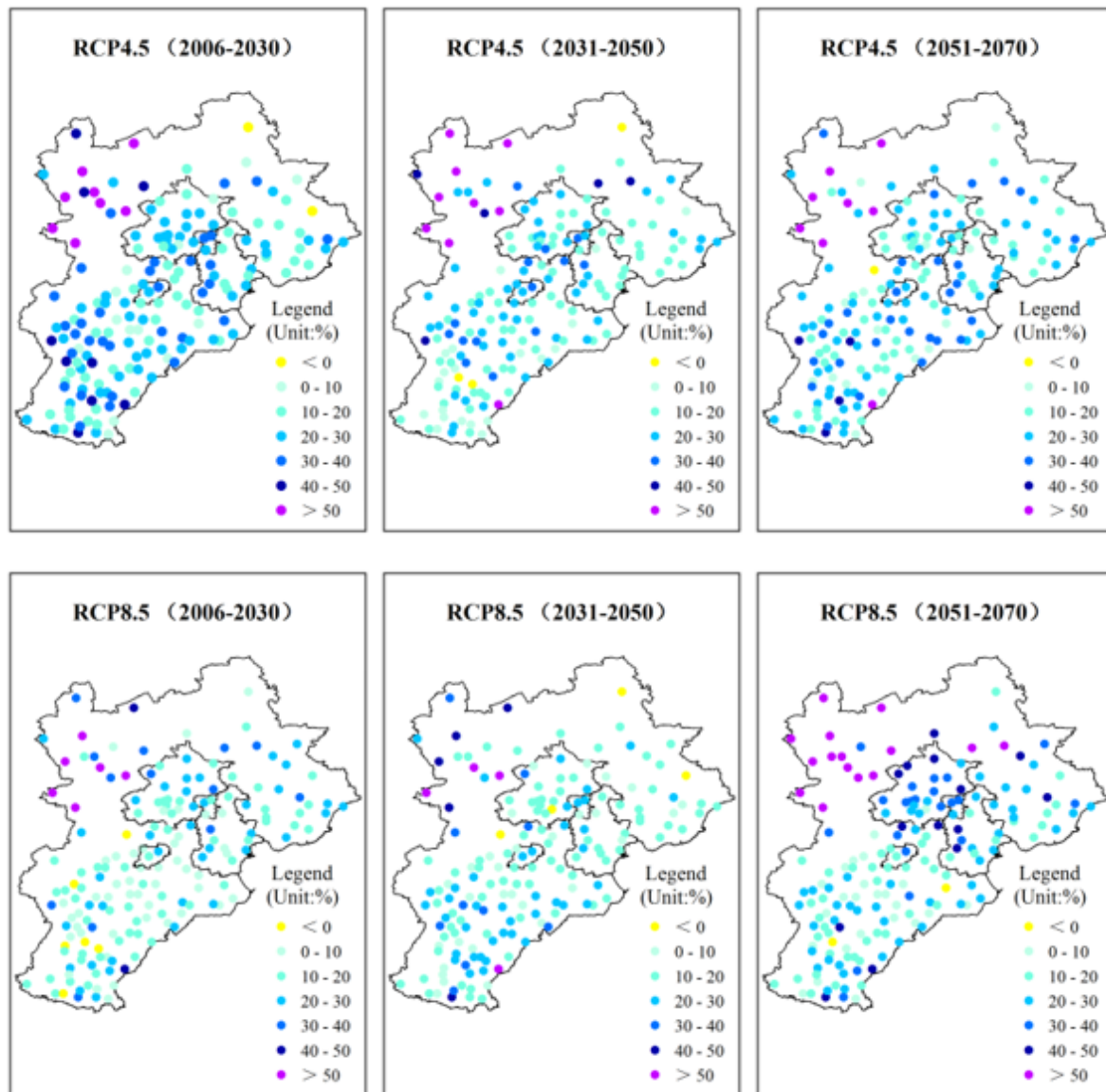
Figure 5. Spatial distribution of annual percentage changes of Exc40 across the Beijing-Tianjin-Hebei region during 2006–2030, 2031–2050, and 2051–2070, compared with 1961–2005.

For Px1d under RCP 4.5, the percentage changes averaged across the Beijing-Tianjin-Hebei region and the five GCMs during 2006–2030, 2031–2050, and 2051–2070 were 12.8%, 8.3%, and 12.6%, respectively. Only the model NorESM1-M in 2031–2050 showed a decreasing trend, which is in contrast to most other GCMs. Under RCP 8.5, the averaged greatest one-day precipitation across the Beijing-Tianjin-Hebei region also showed an increasing trend in the future. However, the changes relative to 1961–2005 during 2006–2030 and 2051–2070 were 10.8% and 8.6%, respectively (less than the increases under RCP 4.5). The change for 2031–2050 was 11.4%, which is more than that under RCP 4.5. Figure 6 shows the spatial distribution of percentage changes of Px1d across the Beijing-Tianjin-Hebei region during the three time periods compared with 1961–2005. The variation in Px1d between stations was larger than that of the former indices, which demonstrates the need for downscaling. The increase at some stations would be more than 40%, while at other stations in the southern and central Beijing-Tianjin-Hebei region, this index is expected to decrease by more than 20%. Specifically, 25.3%, 33.9%, and 29.3% of stations are projected to experience negative changes under RCP 4.5 during 2006–2030, 2031–2050, and 2051–2070, respectively. Furthermore, under RCP 8.5 in the future three periods, nearly one third of

the stations would have negative changes (Table 5). Most of these stations are located in the southern and central Beijing-Tianjin-Hebei region.
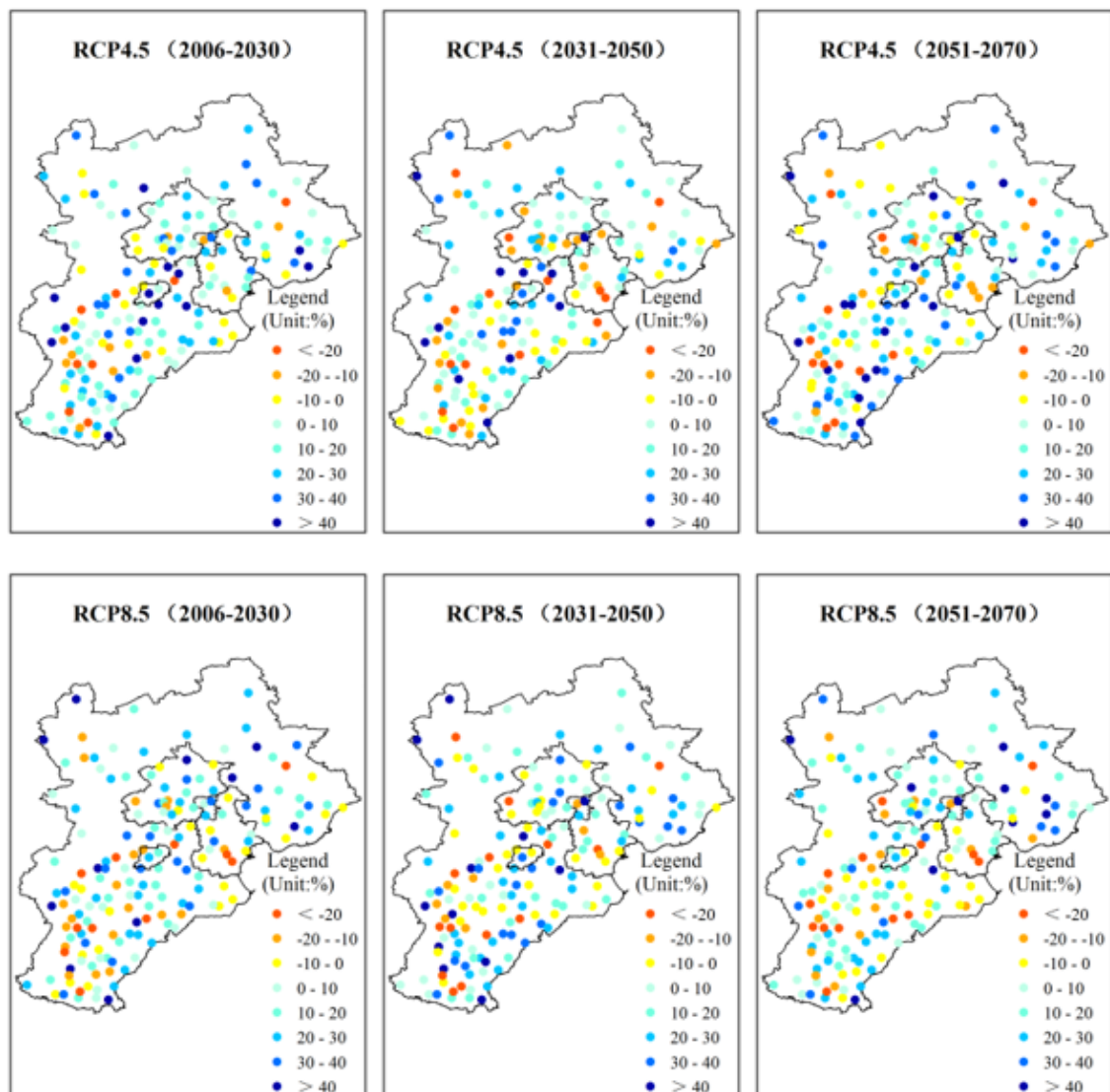
Figure 6. Spatial distribution of annual percentage changes of Px1d across the Beijing-Tianjin-Hebei region during 2006–2030, 2031–2050, and 2051–2070 compared with 1961–2005.

Table 5. The percentages of stations with negative changes in the eight precipitation indices during the future three periods in the Beijing-Tianjin-Hebei region (unit: %).

Time Period	Climate Change Scenario	Arain	Nrain	Pint	Exc25	Exc40	Px1d	Px5d	Pxcdd
2006–2030	RCP4.5	1.1	44.8	0.0	1.1	1.1	25.3	21.8	54.0
	RCP8.5	4.0	32.2	3.4	6.9	3.4	31.6	26.4	52.9
2031–2050	RCP4.5	0.0	33.9	0.0	0.6	1.7	33.9	32.2	53.4
	RCP8.5	2.9	70.7	1.1	2.9	2.3	31.6	25.9	51.7
2051–2070	RCP4.5	0.0	45.4	0.0	0.6	0.6	29.3	24.1	47.7
	RCP8.5	0.0	27.6	0.0	1.1	1.1	33.3	31.6	49.4

For Px5d under RCP 4.5, the average changes across the Beijing-Tianjin-Hebei region downscaled from the simulations of the five GCMs during 2006–2030, 2031–2050, and

2051–2070 were 14.5%, 10.4%, and 14.5% respectively. Only NorESM1-M in 2031–2050 showed a decreasing trend in Px5d, which is contrary to most other GCMs. Under RCP 8.5, the averaged greatest five-day precipitation in the Beijing-Tianjin-Hebei region also showed an increasing trend. However, the projected changes in Px5d were 11.9% and 9.1% during 2006–2030 and 2051–2070, respectively, which were less than those of RCP 4.5. The change for 2031–2050 was 12.3%, greater than that of RCP 4.5. Figure 7 shows the spatial distribution of the percentage changes of Px5d across the Beijing-Tianjin-Hebei region during the three time periods compared with 1961–2005. Similar to Px1d, Px5d showed a large spatial variance. The increase in some stations would be more than 40%, while in some other stations in the southern and central Beijing-Tianjin-Hebei region, the decrease was larger than 20%. The percentages of stations with negative changes under RCP 4.5 during 2006–2030, 2031–2050, and 2051–2070 were 21.8%, 32.2%, and 24.1%, respectively. Under RCP 8.5, the respective percentages of stations with decreasing Px5d were 26.4%, 25.9%, and 31.6% (Table 5).
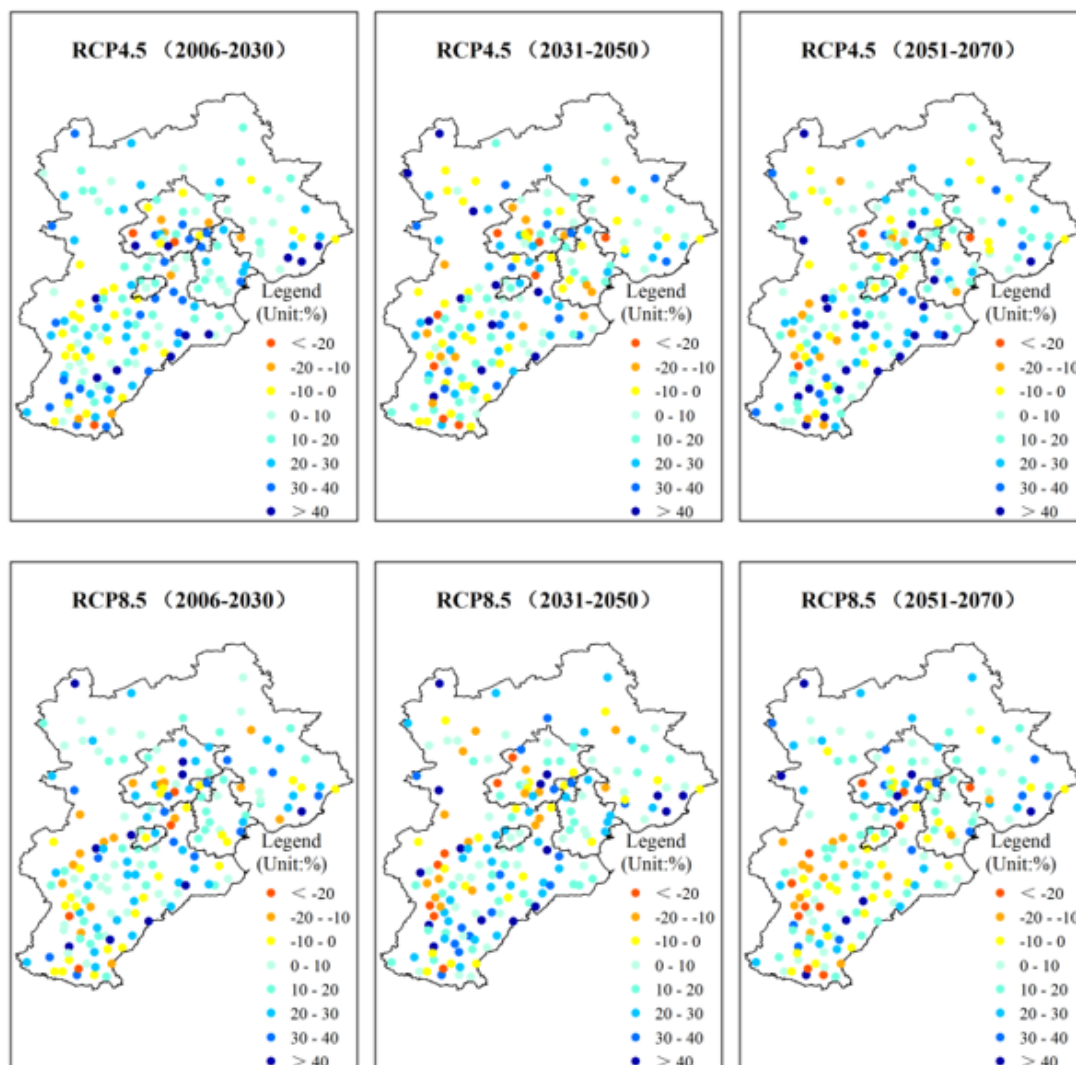
Figure 7. Spatial distribution of annual percentage changes of Px5d across the Beijing-Tianjin-Hebei region during 2006–2030, 2031–2050, and 2051–2070 compared with 1961–2005.

3.4. Changes to Drought Risk

The maximum number of consecutive days without precipitation is a useful indication of drought risk [66,67]. Under RCP 4.5, the five-GCM average changes of Pxcdd across the Beijing-Tianjin-Hebei region during 2006–2030, 2031–2050, and 2051–2070 were −0.3%,

−0.5%, and −0.2%, respectively. Under RCP 8.5, the regional average Pxcdd in the Beijing-Tianjin-Hebei region also showed a decreasing trend, but the range of this change was larger than that under RCP 4.5. Some GCMs predicted an increase, while others predicted a decrease (Table 3). On the whole, the average maximum number of consecutive days without precipitation in the Beijing-Tianjin-Hebei region is expected to decrease. Consequently, the drought risk in this area would slightly decrease. This may be considered a good thing, despite the very small change projected. The Beijing-Tianjin-Hebei Urban Agglomeration belongs to an arid and a semi-arid climate zone and the shortage of water resources is one of the main factors restricting urban development. Unfortunately, the regional average annual Pxcdd in the Xiongan New Area, which is under construction, is expected to increase in the future under both scenarios (Table 4). The risk of drought disaster in this area may further increase. Figure 8 shows the spatial distribution of the percentage changes of Pxcdd across the Beijing-Tianjin-Hebei region during the three periods compared with 1961–2005. The increasing magnitude in some stations was more than 30%, while in some other stations, the decreasing magnitude was less than −30%. The percentages of stations with negative changes under RCP 4.5 during 2006–2030, 2031–2050, and 2051–2070 were 54.0%, 53.5%, and 47.7%, respectively. Under RCP 8.5 in those three future periods, there were 52.9%, 51.7%, and 49.4% of stations with negative changes (Table 5).
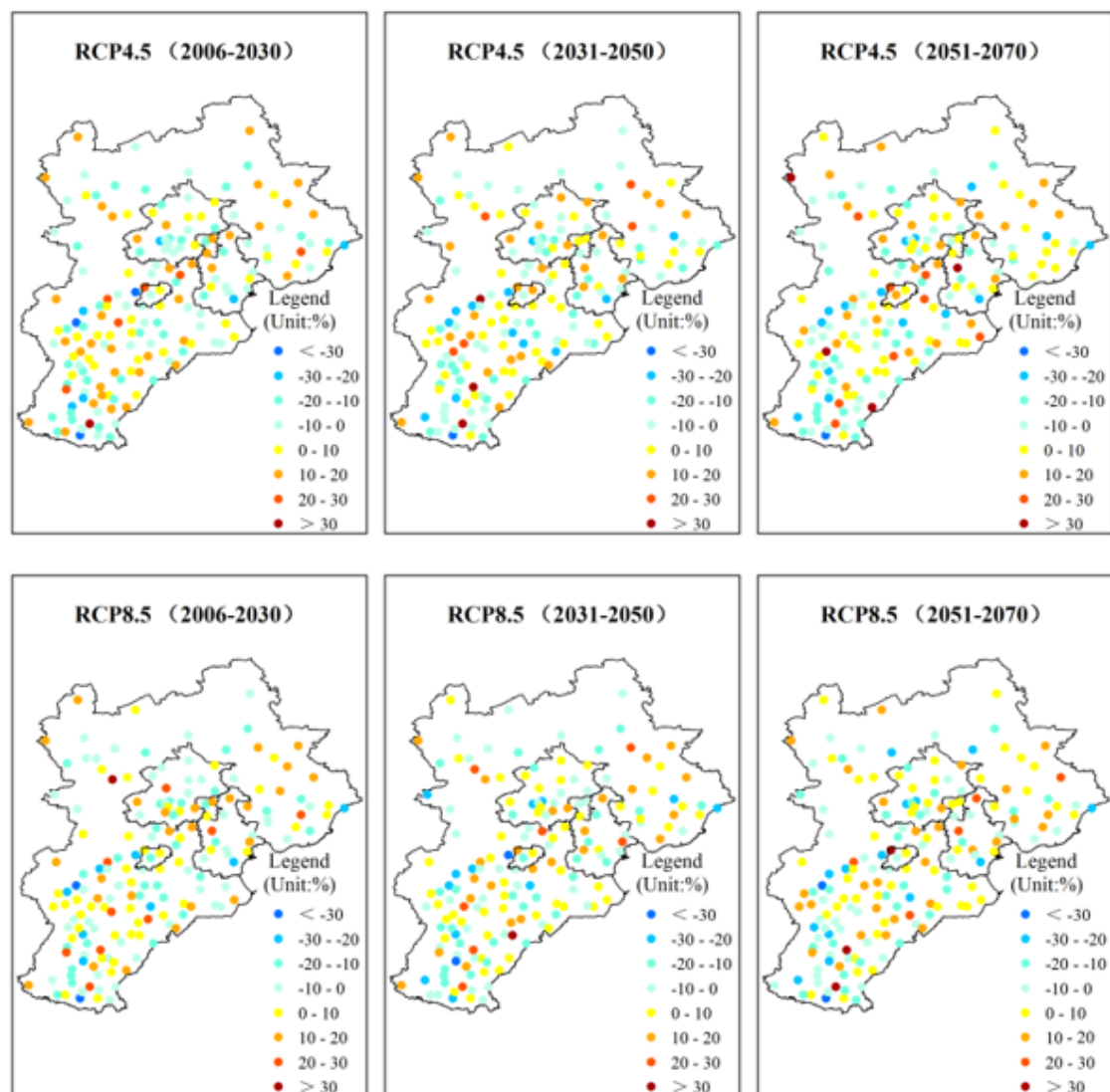
Figure 8. Spatial distribution of annual percentage changes of Pxcdd across the Beijing-Tianjin-Hebei region during 2006–2030, 2031–2050, and 2051–2070 compared with 1961–2005.

4. Conclusions

Future precipitation at the local scale in China's Beijing-Tianjin-Hebei region was projected in this study using a statistical downscaling method with the weather generator BCC/RCG-WG driven by the output of five GCMs. Daily precipitation was simulated for the three periods 2006–2030, 2031–2050, and 2051–2070 at 174 stations in the Beijing-Tianjin-Hebei region. The large-scale climate change signal for the simulations of the future daily local precipitation climate was taken from the five GCMs under the RCP 4.5 and RCP 8.5 emission scenarios. One important objective of this study was to quantify future mean and daily extreme precipitation at the station scale in the Beijing-Tianjin-Hebei region. This was achieved by using eight indices for precipitation. These indices were derived from the simulated daily precipitation at each of the 174 stations during the three periods. The results showed a general trend toward wetter and stronger extremes across the Beijing-Tianjin-Hebei region on an annual scale in the future, and are generally consistent with the large-scale signal from the GCMs. However, the downscaled scenarios showed local-scale variations that could not be captured by the GCMs.

Specifically, the following conclusions can be drawn from this work:

- Compared with the baseline during 1961–2005, the regional average annual precipitation is projected to increase in all three future periods across the Beijing-Tianjin-Hebei region under both RCP 4.5 and RCP 8.5. This increase would be particularly large during 2051–2070 under RCP 8.5, with an increase in 10.3%.
- The projected changes in the number of days with precipitation are relatively small across the Beijing-Tianjin-Hebei region. Regional average Nrain increases by 0.2~1.0% under both RCP 4.5 and RCP 8.5, except during 2031–2050 under RCP 8.5 when it decreases by 0.7%.
- The annual intensity of precipitation at most stations across the Beijing-Tianjin-Hebei region is projected to increase except for some southern stations. Especially in 2051–2070 under RCP 8.5, the intensity would increase by more than 10% at most northern stations.
- There would be more extreme precipitation events across the Beijing-Tianjin-Hebei region in the future. Under RCP 4.5, Exc25 would continually increase across the Beijing-Tianjin-Hebei region. The regional average is projected to increase by 14.8%, 15.0%, and 15.3% during 2006–2030, 2031–2050, and 2051–2070, respectively. In 2051–2070 under RCP 8.5, this change reaches 18.9%. At most northern stations, Exc25 is projected to increase by more than 20%, and even more than 50% at some northwest stations.
- The relative increase in Exc40 is the largest among the eight indices. The regional average annual Exc40 across the Beijing-Tianjin-Hebei region would increase by more than 20% under RCP 4.5. Under RCP 8.5 during 2051–2070, this increase would reach 26.3%.
- Although simulated Px1d and Px5d increase overall in the Beijing-Tianjin-Hebei region, there is high variability among stations, which demonstrates the need for downscaling. These indices would increase at some stations, and decrease at others. The regional average of Px1d and Px5d across the Beijing-Tianjin-Hebei region simulated by the five GCMs presented an increase of 8~15% under both RCP 4.5 and RCP 8.5, and there would be decreases in these indices at 20~35% of the stations in the region.
- Generally, the average Pxcdd in the Beijing-Tianjin-Hebei region is projected to decrease in the future, and the drought risk in this area is expected to decrease. This change may be considered a good thing, despite the very small change projected. However, the consistency of change in Pxcdd between stations is the lowest among the eight indices, and around half of the stations showed negative changes under both RCP 4.5 and RCP 8.5 in the future three periods.

References

1. Zhang, J.; Sun, F.B.; Liu, W.B.; Liu, J.H.; Wang, H. Spatio-temporal patterns of drought evolution over the Beijing-Tianjin-Hebei region, China. *J. Geogr. Sci.* **2019**, *29*, 863–876. [CrossRef]
2. Lin, X.H.; Peng, X.; Li, X.J. A study of the characteristics of coastal economic development in China under the new situation. *Mar. Econ.* **2019**, *9*, 12–19.
3. Chen, J. Xiongan New Area: New highland of global innovation. *Bull. Chin. Acad. Sci.* **2017**, *32*, 1256–1259.
4. Han, H.; Gong, D.Y. Extreme climate events over northern China during the last 50 years. *J. Geogr. Sci.* **2003**, *13*, 469–479.
5. Yang, W.X.; Li, H.Y.; Zhang, G.H.; Li, Z.T. Analysis on vapor field for the drought causes in Beijing, Tianjin and Hebei districts in recent years. *Agric. Sci. Technol.* **2010**, *11*, 117–121.
6. Chi, Y.Y.; Xu, K.P.; Wang, J.J.; Zhang, L.P. Identifying regional ecological space in Beijing, Tianjin, and Hebei. *Acta Ecol. Sin.* **2018**, *38*, 8555–8563.
7. Song, X.M.; Zou, X.J.; Zhang, C.H.; Zhang, J.Y.; Kong, F.Z. Multiscale spatio-temporal changes of precipitation extremes in Beijing-Tianjin-Hebei region, China during 1958–2017. *Atmosphere* **2019**, *10*, 462. [CrossRef]
8. Liao, Y.M.; Huang, D.P. Climate characteristics and change trend of Xiongan New area. *Chin. Agric. Sci. Bull.* **2020**, *36*, 99–105.
9. Xing, C.G.; Zhao, S.Q.; Yan, H.M.; Yang, H.C. Ecological compensation mechanism for Beijing-Tianjin-Hebei region based on footprint balance and footprint deficit. *Ecol. Econ.* **2020**, *16*, 218–229.
10. Zhang, K.H. The impacts of global climate change on extreme weather events in Beijing-Tianjin-Hebei area and the countermeasures for disaster prevention. *J. Arid Land Resour. Environ.* **2011**, *25*, 122–125.
11. Shi, Y.; Han, Z.Y.; Xu, Y.; Zhou, B.T.; Wu, J. Future changes of climate extremes in Xiongan New Area and Jing-Jin-Ji district based on high resolution (6.25 km) combined statistical and dynamical downscaling datasets. *Clim. Change Res.* **2019**, *15*, 140–149.
12. Wang, H.J.; Sun, J.Q.; Chen, H.P.; Zhu, Y.L.; Zhang, Y.; Jiang, D.B.; Lang, X.M.; Fan, K.; Yu, E.T.; Yang, S. Extreme Climate in China: Facts, Simulation and Projection. *Meteorol. Z.* **2012**, *21*, 279–304. [CrossRef]
13. Ou, T.; Chen, D.; Linderholm, H.W.; Jeong, J.H. Evaluation of global climate models in simulating extreme precipitation in China. *Tellus A Dyn. Meteorol. Oceanogr.* **2013**, *65*, 1393–1399. [CrossRef]
14. Ji, Z.M.; Kang, S.C. Evaluation of extreme climate events using a regional climate model for China. *Int. J. Climatol.* **2014**, *35*, 888–902. [CrossRef]
15. Li, W.; Jiang, Z.H.; Zhang, X.B.; Li, L.; Sun, Y. Additional risk in extreme precipitation in China from 1.5 °C to 2.0 °C global warming levels. *Sci. Bull.* **2018**, *63*, 228–234. [CrossRef]
16. Meng, C.C.; Zhang, L.; Gou, P.; Huang, Q.Q.; Ma, Y.M.; Miao, S.G.; Ma, W.Q.; Xu, Y.L. Assessments of future climate extremes in China by using high-resolution PRECIS 2.0 simulations. *Theor. Appl. Climatol.* **2021**, *145*, 295–311. [CrossRef]
17. Wei, W.; Shi, Z.J.; Yang, X.H.; Wei, Z.; Liu, Y.S.; Zhang, Z.Y.; Ge, G.; Zhang, X.; Guo, H.; Zhang, K.B.; et al. Recent Trends of Extreme Precipitation and Their Teleconnection with Atmospheric Circulation in the Beijing-Tianjin Sand Source Region, China, 1960–2014. *Atmosphere* **2017**, *8*, 83. [CrossRef]
18. Schoof, J.T. Statistical downscaling in climatology. *Geogr. Compass* **2013**, *7*, 249–265. [CrossRef]
19. Winkler, J.A.; Guentchev, G.S.; Liszewska, M.; Perdinan; Tan, P.N. Climate scenario development and applications for local/regional climate change impact assessments: An overview for the non-climate scientist. *Geogr. Compass* **2011**, *5*, 301–328. [CrossRef]
20. Feng, J.M.; Wang, Y.L.; Fu, C.B. Simulation of extreme climate events over China with different regional climate models. *Atmos. Ocean. Sci. Lett.* **2011**, *4*, 47–56.

21. Jiang, Z.H.; Song, J.; Li, L.; Chen, W.L.; Wang, Z.F.; Wang, J. Extreme climate events in China: IPCC-AR4 model evaluation and projection. *Clim. Chang.* **2012**, *110*, 385–401. [CrossRef]

22. Gao, X.J.; Wang, M.L.; Giorgi, F. Climate change over China in the 21st century as simulated by BCC_CSM1.1-RegCM4.0. *Atmos. Ocean. Sci. Lett.* **2013**, *6*, 381–386.

23. Zou, L.W.; Zhou, T.J. Near future (2016–2040) summer precipitation changes over China as projected by a regional climate model (RCM) under the RCP8.5 emissions scenario: Comparison between RCM downscaling and the driving GCM. *Adv. Atmos. Sci.* **2013**, *30*, 806–818. [CrossRef]

24. Yang, S.L.; Feng, J.M.; Dong, W.J.; Chou, J.M. Analyses of extreme climate events over China based on CMIP5 historical and future simulations. *Adv. Atmos. Sci.* **2014**, *31*, 1209–1220. [CrossRef]

25. Xu, Y.; Wu, J.; Shi, Y.; Zhou, B.T.; Li, R.K.; Wu, J. Change in extreme climate events over China based on CMIP5. *Atmos. Ocean. Sci. Lett.* **2015**, *8*, 185–192.

26. Wang, Y.J.; Zhou, B.T.; Qin, D.H.; Wu, J.; Gao, R.; Song, L.C. Changes in mean and extreme temperature and precipitation over the arid region of northwestern China: Observation and projection. *Adv. Atmos. Sci.* **2017**, *34*, 289–305. [CrossRef]

27. Wang, K.; Shi, H.D.; Gao, J.J.; Wang, C.L.; Hua, S.B.; Gao, Q.X. Potential variation of Beijing-Tianjin-Hebei Region's air quality in RCP 8.5 scenarios by dynamic downscaling method with CCSM4/wrf-CMAQ model. *Res. Environ. Sci.* **2017**, *30*, 1661–1669.

28. Han, Z.Y.; Tong, Y.; Gao, X.J.; Xu, Y. Correction based on quantile mapping for temperature simulated by the RegCM4. *Adv. Clim. Change Res.* **2018**, *14*, 331–340.

29. Wu, J.; Gao, X.J.; Xu, Y. Climate change projection over Xiong'an District and its adjacent areas: An ensemble of RegCM4 simulations. *Chin. J. Atmos. Sci.* **2018**, *42*, 696–705.

30. Wei, L.X.; Xin, X.G.; Xiao, C.; Li, Y.H.; Wu, Y.; Tang, H.Y. Performance of BCC-CSM models with different horizontal resolutions in simulating extreme climate events in China. *J. Meteorol. Res.* **2019**, *33*, 720–733. [CrossRef]

31. Li, R.K.; Han, Z.Y.; Xu, Y.; Shi, Y.; Wu, J. An ensemble projection of GDP and population exposure to high temperature events over Jing–Jin–Ji district based on high resolution combined dynamical and statistical downscaling datasets. *Clim. Chang. Res.* **2020**, *16*, 491–504.

32. Zhang, D.F.; Gao, X.J. Climate change of the 21st century over China from the ensemble of RegCM4 simulations. *Chin. Sci. Bull.* **2020**, *65*, 2516–2526. [CrossRef]

33. Han, Z.Y.; Shi, Y.; Wu, J.; Xu, Y. Combined dynamical and statistical downscaling for high-resolution projections of multiple climate variables in the Beijing-Tianjin-Hebei region of China. *J. Appl. Meteorol. Climatol.* **2019**, *58*, 2387–2403. [CrossRef]

34. Wang, Y.J.; Song, L.C.; Han, Z.Y.; Liao, Y.M.; Xu, H.M.; Zhai, J.Q.; Zhu, R. Climate-related risks in the construction of Xiongan New Area, China. *Theor. Appl. Climatol.* **2020**, *141*, 1301–1311. [CrossRef]

35. Fan, L.J.; Fu, C.B.; Chen, D. Review on creating future climate change scenarios by statistical downscaling techniques. *Adv. Earth Sci.* **2005**, *20*, 320–329.

36. Xu, Z.; Han, Y.; Yang, Z. Dynamical downscaling of regional climate: A review of methods and limitations. *Sci. China Earth Sci.* **2019**, *62*, 365–375. [CrossRef]

37. Chen, D.; Achberger, C.; Räisänen, J.; Hellström, C. Using statistical downscaling to quantify the GCM-related uncertainty in regional climate change scenarios: A case study of Swedish precipitation. *Adv. Atmos. Sci.* **2006**, *23*, 54–60. [CrossRef]

38. Wilks, D.S.; Wilby, R.L. The weather generation game: A review of stochastic weather models. *Prog. Phys. Geogr.* **1999**, *23*, 329–357. [CrossRef]

39. Kilsby, C.G.; Jones, P.D.; Burton, A.; Ford, A.C.; Fowler, H.J.; Harpham, C.; James, P.; Smith, A.; Wilby, R.L. A daily weather generator for use in climate change studies. *Environ. Model. Softw.* **2007**, *22*, 1705–1719. [CrossRef]

40. Jones, P.D.; Harpham, C.; Goodess, C.M.; Kilsby, C.G. Perturbing a weather generator using change factors derived from regional climate model simulations. *Nonlinear Processes Geophys.* **2011**, *18*, 503–511. [CrossRef]

41. Taylor, K.E.; Stouffer, R.J.; Meehl, G.A. An overview of CMIP5 and the experiment design. *Bull. Am. Meteorol. Soc.* **2012**, *93*, 485–498. [CrossRef]

42. Zhou, W.C.; Han, Z.Y. Assessing CMIP5 climate simulations and objective selection of models over the Yellow River basin. *J. Meteorol. Environ.* **2018**, *34*, 42–55.

43. Alexander, L.V.; Zhang, X.; Peterson, T.C.; Caesar, J.; Gleason, B.; Klein-Tank, A.M.G.; Haylock, M.; Collins, D.; Trewin, B.; Rahimzadeh, F.; et al. Global observed changes in daily climate extremes of temperature and precipitation. *J. Geophys. Res.* **2006**, *111*, D05109.

44. Chen, D.; Achberger, C.; Ou, T.; Postgård, U.; Walther, A.; Liao, Y.M. Projecting future local precipitation and its extremes for Sweden. *Geogr. Ann. Ser. A Phys. Geogr.* **2015**, *97*, 25–39. [CrossRef]

45. Liao, Y.M.; Zhang, Q.; Chen, D. Stochastic modeling of daily precipitation in China. *J. Geogr. Sci.* **2004**, *14*, 417–426.

46. Liao, Y.M.; Chen, D.; Gao, G.; Xie, Y. Impacts of climate changes on parameters of a weather generator for daily precipitation in China. *Acta Geogr. Sin.* **2009**, *64*, 871–878.

47. Liao, Y.M.; Liu, L.L.; Chen, D.; Xie, Y. An evaluation of the BCC/RCG-WG's performance in simulating daily non-precipitation variables in China. *Acta Meteorol. Sin.* **2011**, *69*, 310–319.

48. Liao, Y.M.; Chen, D.; Xie, Y. Spatial variability of the parameters of the Chinese stochastic weather generator for daily non-precipitation variables simulation in China. *Acta Meteorol. Sin.* **2013**, *71*, 1103–1114.

49. Liao, Y.M. Change of parameters of BCC/RCG-WG for daily non-precipitation variables in China: 1951–1978 and 1979–2007. *J. Geogr. Sci.* **2013**, *23*, 579–594.

50. Wight, J.R.; Hanson, C.L. Use of stochastically generated weather records with rangeland simulation models. *J. Range Manag.* **1991**, *44*, 282–285. [CrossRef]

51. Semenov, M.A.; Brooks, R.J. Spatial interpolation of the LARS-WG stochastic weather generator in Great Britain. *Clim. Res.* **1999**, *11*, 137–148. [CrossRef]

52. Hay, L.E.; Wilby, R.L.; Leavesley, G.H. A comparison of delta change and downscaled GCM scenarios for three mountainous basins in the United States. *J. Am. Water Resour. Assoc.* **2000**, *36*, 387–397. [CrossRef]

53. Wilks, D.S. Use of stochastic weather generators for precipitation downscaling. *Wiley Interdiscip. Rev. Clim. Change* **2010**, *1*, 898–907. [CrossRef]

54. Yang, W.; Andréasson, J.; Graham, L.P.; Olsson, J.; Rosberg, J.; Wetterhall, F. Distribution-based scaling to improve usability of regional climate model projections for hydrological climate change impacts studies. *Hydrol. Res.* **2010**, *41*, 211–229. [CrossRef]

55. Semenov, M.A.; Porter, J.R. Climatic variability and the modelling of crop yields. *Agric. For. Meteorol.* **1995**, *173*, 265–283. [CrossRef]

56. Li, P.F.; Liu, W.J.; Zhao, X.Y. The changes of atmospheric temperature, precipitation and potential evapotranspiration in Beijing-Tianjin-Hebei region in recent 50 years. *J. Arid Land Resour. Environ.* **2015**, *29*, 137–143.

57. Yu, Z.J.; Jin, Z.; Zhang, Y.P. Analysis on the change characteristics of precipitation in Beijing-Tianjin-Hebei region in recent 56 years. *J. Anhui Agric. Sci.* **2019**, *47*, 215–221.

58. Miao, Z.W.; Li, N.; Lu, M.; Xu, L.G. Variation characteristics of extreme precipitation event in Beijing-Tianjin-Hebei region during 1961–2017. *Water Resour. Hydropower Eng.* **2019**, *50*, 34–44.

59. Feng, L.; Zhou, T.J.; Wu, B.; Li, T.; Luo, J.J. Projection of future precipitation change over China with a high-resolution global atmospheric model. *Adv. Atmos. Sci.* **2011**, *28*, 464–476. [CrossRef]

60. Zhang, Y.W.; Jiang, F.Q.; Wei, W.S.; Liu, M.Z.; Wang, W.W.; Bai, L.; Li, X.H.; Wang, S. Changes in annual maximum number of consecutive dry and wet days during 1961–2008 in Xinjiang, China. *Nat. Hazards Earth Syst. Sci.* **2012**, *12*, 1353–1365. [CrossRef]

61. Gao, H.; Jiang, W.; Li, W.J. Changed relationships between the East Asian summer monsoon circulations and the summer rainfall in eastern China. *J. Meteorol. Res.* **2014**, *28*, 1075–1084. [CrossRef]

62. Zhang, R.H. Natural and human-induced changes in summer climate over the East Asian monsoon region in the last half century: A review. *Adv. Clim. Chang. Res.* **2015**, *6*, 131–140. [CrossRef]

63. Hao, L.S.; Ding, Y.H.; Min, J.Z. Relationship between summer monsoon changes in East Asia and abnormal summer rainfall in North China. *Plateau Meteorol.* **2016**, *35*, 1280–1289.

64. Wang, G.M.; Liu, L.Y.; Hu, Z.Y. Risk assessment of rainstorm and flood disasters at grid-scale in Beijing-Tianjin-Hebei metropolitan area. *J. Catastropho.* **2020**, *35*, 186–193.

65. Chen, H.P.; Sun, J.Q.; Li, H.X. Future changes in precipitation extremes over China using the NEX-GDDP high-resolution daily downscaled data-set. *Atmos. Ocean. Sci. Lett.* **2017**, *10*, 403–410. [CrossRef]

66. Zhang, D.F.; Shi, Y. Numerical simulation of climate changes over North China by RegCM3 model. *Chin. J. Geophys.* **2012**, *55*, 2854–2866. [CrossRef]

67. Duan, Y.W.; Ma, Z.G.; Yang, Q. Characteristics of consecutive dry days variations in China. *Theor. Appl. Climatol.* **2017**, *130*, 701–709. [CrossRef]